Mathematical Biosciences 300 (2018) 130–137

Contents lists available at ScienceDirect

Mathematical Biosciences

journal homepage: www.elsevier.com/locate/mbs

Homeostasis despite instability

W. Duncan[a], J. Best[b], M. Golubitsky[b], H.F. Nijhout[c], M. Reed[*,a]

[a] Department of Mathematics, Duke University, Durham, NC 27708, USA
[b] Department of Mathematics, The Ohio State University, Columbus, OH 43210, USA
[c] Department of Biology, Duke University, Durham, NC 27708, USA

ARTICLE INFO

Keywords:
Biochemistry
Homeostasis
Chair curve
Instability
Feedback inhibition

ABSTRACT

We have shown previously that different homeostatic mechanisms in biochemistry create input-output curves with a "chair" shape. At equilibrium, for intermediate values of a parameter (often an input), a variable, Z, changes very little (the homeostatic plateau), but for low and high values of the parameter, Z changes rapidly (escape from homeostasis). In all cases previously studied, the steady state was stable for each value of the input parameter. Here we show that, for the feedback inhibition motif, stability may be lost through a Hopf bifurcation on the homeostatic plateau and then regained by another Hopf bifurcation. If the limit cycle oscillations are relatively small in the unstable interval, then the variable Z maintains homeostasis despite the instability. We show that the existence of an input interval in which there are oscillations, the length of the interval, and the size of the oscillations depend in interesting and complicated ways on the properties of the inhibition function, f, the length of the chain, and the size of a leakage parameter.

1. Introduction

Most human and animal physiological systems can function well in the face of gene polymorphisms and changes in the environment because of rich networks of regulatory mechanisms. This is true at all levels of organization, from gene networks, to cellular biochemistry, to tissue and organ properties, and to the behavior of the whole organism. In the simplest case, this is illustrated conceptually by the function $Z(I)$ in Fig. 1. The variable Z depends on I, which could represent an input, an environmental variable, or some other variable of the system. However, over a large range of I (between $H_1 = 6$ and $H_2 = 15$ in Fig. 1), the value of $Z(I)$ changes very little. The homeostatic region is the range of I where $Z(I)$ changes very little. Outside the homeostatic region the regulatory mechanisms fail and $Z(I)$ changes rapidly as I varies; we call this escape from homeostasis [1]. Overall the curve giving the dependence looks like a chair [2], and examples of such chair curves abound: body temperature as a function of environmental temperature [1]; liver homocysteine concentration as a function of methionine input [1]; afferent arterial flow in the kidney as a function of blood pressure [3]; cerebral blood flow as a function of cerebral blood pressure [4]. In studying metabolism, we have found that many different kinds of biochemical mechanisms can produce chair curves [5]. Golubitsky and Stewart have used singularity theory as an analytical tool to find nodes in networks that are homeostatic with respect to an input [6].

We have investigated [5] many different biochemical mechanisms that give rise to homeostasis where, typically, I is an input to the network. In all of these cases, the system had a unique stable equilibrium for each I. In this paper we show an entirely new phenomenon. The steady state of the system can lose its stability, yet the system still shows a homeostatic region and a chair curve. Consider the simple biochemical chain pictured in Fig. 2. The last element in the chain, X_n, inhibits the reaction that takes X_1 to X_2. This kind of feedback inhibition is one of the most common homeostatic mechanisms in biochemistry [5]. The homeostatic variable is X_n because as I increases, X_n tends to increase, which increases the inhibition by f, limiting how much X_n rises.

For $n = 4$ and an appropriate choice of the inhibitory function, f, the system shows the behavior indicated in Fig. 3. For I small, the equilibrium is stable and $X_4(I)$ increases linearly in I. At the value I_1 there is a Hopf bifurcation and the equilibrium becomes unstable but shows homeostasis (the red curve). Finally at I_2, the equilibrium becomes stable again and shortly thereafter $X_4(I)$ shows escape from homeostasis by rising linearly with I. For I in the interval (I_1, I_2), the system has a stable limit cycle; the green curves show the maximum and minimum values of $X_4(I, t)$ as $X(I, t)$ traverses the limit cycle for fixed I.

Consider biological experiments on this system where the experimenter chooses an input, I, and then measures X_4. When $I < I_1$, the measurements will cluster tightly about the stable equilibria on the blue curve. For $I_1 < I < I_2$, there will be more spread of the measured values because X_4 is changing in time because the dynamics has a limit cycle.

* Corresponding author.
E-mail address: reed@math.duke.edu (M. Reed).

https://doi.org/10.1016/j.mbs.2018.03.025
Received 8 December 2017; Received in revised form 23 March 2018; Accepted 24 March 2018
Available online 27 March 2018
0025-5564/ © 2018 Elsevier Inc. All rights reserved.

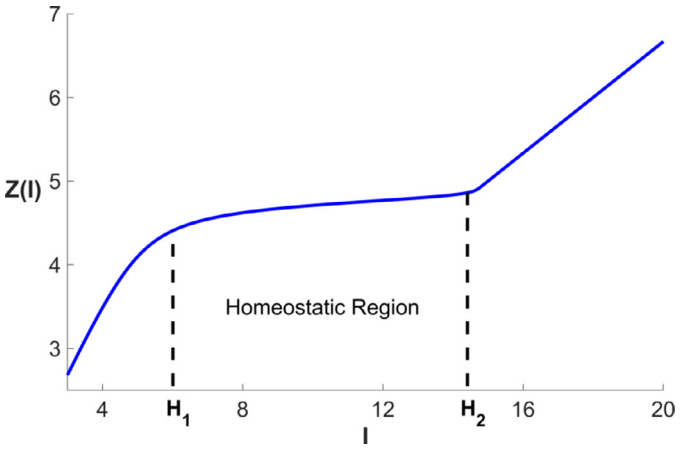

Fig. 1. A classic chair curve. The variable Z shows homeostasis and escape from homeostasis with respect to the variable I.

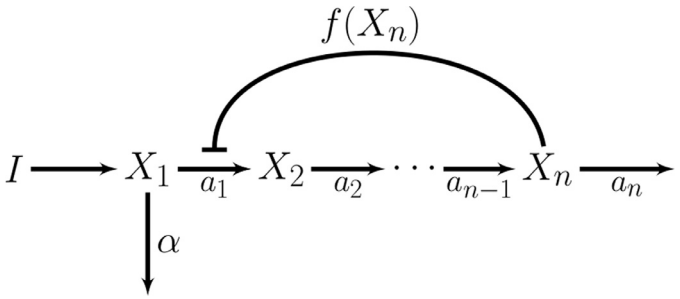

Fig. 2. A simple biochemical chain with feedback inhibition. The variable X_n inhibits the reaction that takes X_1 to X_2 via the function $f(X_n)$. I is the input to the chain.

The spread of the measured values of X_4 will be between the upper and lower green curves (except for measurement error). When $I > I_2$, the measurements will again cluster tightly about the stable equilibria on the blue curve. The experimenter may not know of the existence of the limit cycles, but will notice that there is more spread of the measured values of X_4 when $I_1 < I < I_2$. Since the upper and lower green curves are close to each other, the total set of measured values of X_4, over a wide range of choices of I, will show the same general shape of a chair curve with a homeostatic region in the middle. This is what we mean by "homeostasis despite instability."

In Section 2, we investigate how the phenomenon of homeostasis despite instability depends on network length, n, properties of the feedback function, f, and the value of α. In Section 3, we assume that f has a special form depending on only three parameters, the slope of f, the minimum of f, and the location of the region with constant negative slope. We present numerical calculations that show how the size of the unstable region and the amplitude of the limit cycles depend on these three parameters. In the Discussion, we explain that another homeostatic motif, the parallel inhibition motif [5], shows similar behavior, so homeostasis despite instability is not limited to the feedback inhibition motif.

2. Dependence of stability on network length

Throughout this section we make the following assumptions about f:

$$f \text{ is differentiable, } f > 0, \text{ and } f' \leq 0. \tag{1}$$

We assume $f > 0$ so that the backwards reaction of $X_2 \to X_1$ does not occur and the forward reaction of $X_1 \to X_2$ always occurs at some rate. The assumption that $f' \leq 0$ is made so that X_n inhibits the production of X_2 from X_1. Additionally, we assume $a_j > 0$ for each j. Other hypotheses will be introduced as appropriate. Let $x_i(t)$ denote the concentration of X_i at time t. Each differential equation expresses that the rate of change of the variable is the rate at which it is made minus the rate at which it is consumed. We assume mass action kinetics for all reactions except for the rate from X_1 to X_2 that depends on inhibition from X_n expressed through f. The dynamics are given by

$$\begin{aligned}
\dot{x}_1 &= I - (a_1 f(x_n) + \alpha)x_1 \\
\dot{x}_2 &= a_1 f(x_n)x_1 - a_2 x_2 \\
\dot{x}_3 &= a_2 x_2 - a_3 x_3 \\
&\vdots \\
\dot{x}_n &= a_{n-1}x_{n-1} - a_n x_n
\end{aligned}$$

where dot indicates a derivative in t. When $\alpha = a_2$, $\dot{x}_1 + \dot{x}_2 = I - a_2(x_1 + x_2)$ so that as $t \to \infty$, $x_1 + x_2 \to I/a_2$. This allows us to reduce the dimension of the steady state Jacobian by 1 and to significantly simplify the analysis. We are interested in how n and the properties of f affect the stability of equilibrium solutions to this system. For $n = 2$, 3, and4, we are able to characterize when an equilibrium is stable, and we can do the same for $n = 5$ if $\alpha = 1$. For general n, we give a necessary condition for instability and a sufficient condition for instability, but neither is necessary and sufficient.

Using the equations above, it is easy to see that the steady state solutions satisfy:

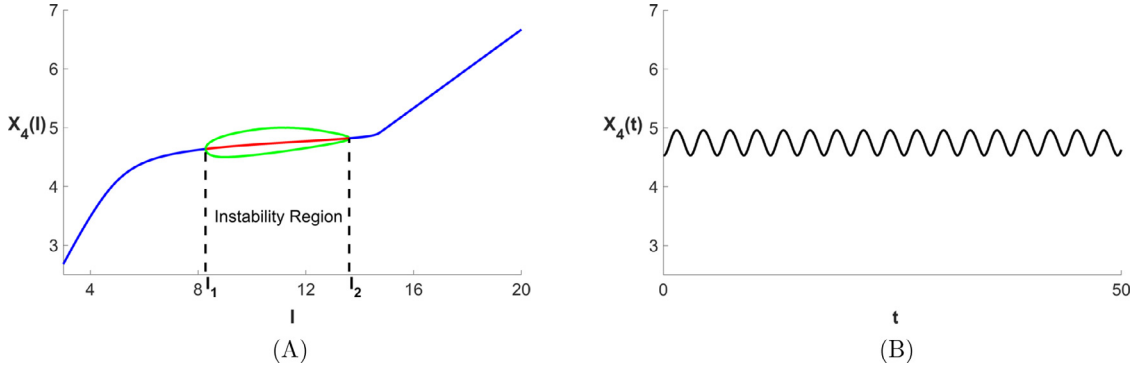

Fig. 3. Homeostasis despite instability. In the feedback chain in Fig. 2, the equilibrium becomes unstable for I in the interval (I_1, I_2) for an appropriate choice of the feedback function f. We chose $n = 4$, $\alpha = 1$, $a_j = 1$ for each j, and $f(x) = 10e^{-1/(5-x)+1/5}\Theta(5-x) + 1/2$, where $\Theta(x)$ is the Heaviside step function. In Panel A, the blue and red curves show the values of $X_4(I)$ at the stable and unstable equilibria, respectively. The green curves show the maximum and minimum values of X_4 as the dynamics traverses the limit cycle for fixed I. Since the green curves are close to each other, experimental measurements (see text) will follow the shape of the curve of equilibria despite the instability. In Panel B we show the time course of the oscillations in X_4 for $I = 10$, where the maximum amplitude oscillations are obtained. (For interpretation of the references to color in this figure legend, the reader is referred to the web version of this article.)

$$\begin{aligned}\overline{x}_1 &= \frac{I}{a_1 f(\overline{x}_n) + \alpha} \\ \overline{x}_j &= \frac{1}{a_j}\frac{a_1 f(\overline{x}_n) I}{a_1 f(\overline{x}_n) + \alpha} \quad \text{for } j \geq 2.\end{aligned} \tag{2}$$

Lemma 1. *Suppose f satisfies (1). Then for each* $I \in [0, \infty)$, *(2) has a unique solution.*

Proof. Let $h(x) = (a_1 f(x) + \alpha)(a_n x)/(a_1 f(x))$ so that $h(\overline{x}_n) = I$. By the hypotheses on f, $h(x)$ is strictly monotone increasing, $h(0) = 0$ and $h(x) \to \infty$ as $x \to \infty$. Thus, h: $[0, \infty) \to [0, \infty)$ is invertible, so that $\overline{x}_n$ is determined by I. For $j < n$, each is an explicit function of $\overline{x}_n$ and I and is thus determined. □

From now on, we drop the overbar and denote $x_j = x_j(I)$ as the steady state concentration of X_j. Except in Theorem 1, we consider only $a_j = 1$ for each j. We are interested in the value of x_n and the stability of the equilibrium. As (2) shows, x_n depends only on a_1 and a_n. The value of a_n scales x_n, so varying a_n leaves the range of homeostasis unchanged. Changing a_1 is equivalent to rescaling $f(x)$, so nothing is lost by setting $a_1 = 1$. We choose $a_j = 1$ for $j = \{2, ..., n-1\}$ for simplicity. Choosing other values makes the proofs more complicated and the statements of some inequalities a little different, but involves no new ideas. We will see later that the choice of α does make a difference.

Differentiating the steady state equation for x_n with respect to I and using (1), we have, for $a_j = 1$,

$$x_n'(I) = \frac{f(x_n)(f(x_n) + \alpha)}{(f(x_n) + \alpha)^2 - \alpha f'(x_n) I} \tag{3}$$

so that $x_n'(I) > 0$ for every I. Although $x_n'(I)$ is always nonzero, it may be small over a range of I so that x_n exhibits a homeostatic region. We will show in the theorems below that if $|f'(x_n)I|$ is large, then the equilibrium is unstable and if $|f'(x_n)I|$ is small, then the equilibrium is stable. Together with (3), this suggests that the homeostatic region and region of instability overlap, as depicted in Fig. 3.

The characteristic polynomial of the Jacobian when all $a_j = 1$ is given by

$$P_n(\lambda) = (f(x_n) + \alpha + \lambda)(1 + \lambda)^{n-1} - f'(x_n) I \left(\frac{\lambda + \alpha}{f(x_n) + \alpha}\right). \tag{4}$$

Expanding, this may also be written as

$$\begin{aligned}P_n(\lambda) = {} & \lambda^n + \sum_{k=2}^{n-1} \left[\binom{n-1}{k} (f(x_n) + \alpha) + \binom{n-1}{k-1} \right] \lambda^k \\ & + \left[(n-1)(f(x_n) + \alpha) + 1 - \frac{f'(x_n) I}{f(x_n) + \alpha} \right] \lambda \\ & + \left[f(x_n) + \alpha - f'(x_n) I \frac{\alpha}{f(x_n) + \alpha} \right].\end{aligned}$$

Note that every coefficient of P_n is positive (since $f' \leq 0$), so that, by Descartes' rule of signs, there can be no real positive roots of P_n. In addition, $\lambda = 0$ is never a root, so a loss of stability must occur by a pair of eigenvalues crossing the imaginary axis, that is, via a Hopf bifurcation.

When $\alpha = 1$, $\lambda = -1$ is always a root of $P_n(\lambda)$. This is a reflection of the fact that $x_1 + x_2 = I$, mentioned above. Dividing out the factor of $(1 + \lambda)$ gives us the characteristic polynomial for the reduced Jacobian:

$$\widetilde{P}_n(\lambda) = (f(x_n) + 1 + \lambda)(1 + \lambda)^{n-2} - \frac{f'(x_n) I}{f(x_n) + 1}$$

Expanded, this is

$$\begin{aligned}\widetilde{P}_n(\lambda) = {} & \lambda^{n-1} + \sum_{k=1}^{n-2} \left[\binom{n-2}{k} (f(x_n) + 1) + \binom{n-2}{k-1} \right] \lambda^k + f(x_n) + 1 \\ & - \frac{f'(x_n) I}{f(x_n) + 1}.\end{aligned}$$

We first study the case when $n \leq 5$. Theorems 1 and 2 together show that $n = 4$ is the minimum network length for which instabilities can occur.

Theorem 1. *Let f satisfy (1). If* $n = 2$ *or 3 and* $\alpha > 0$ *then the equilibrium is locally asymptotically stable for every* $I \in [0, \infty)$.

Proof. Consider $n = 3$. Although the theorem is true for general $\alpha > 0$, we prove it in the case $\alpha = a_2$ only. The technique for the general case is the same as the technique for the $\alpha = 1$, $n = 4$ case used in the proof of Theorem 2.

When $n = 3$ and $\alpha = a_2$, using $x_1 = I/a_2 - x_2$, the reduced Jacobian is given by

$$J = \begin{pmatrix} -(a_1 f(x_3) + a_2) & a_1 f'(x_3)(I/a_2 - x_2) \\ a_2 & -a_3 \end{pmatrix}$$

Since $I/a_2 - x_2 > 0$ and (1) holds, we see $\mathrm{Tr}(J) < 0$ and $\det(J) > 0$ for each choice of $I \geq 0$, so that the steady state is asymptotically stable for every $I \geq 0$. For the case $n = 2$, and $\alpha > 0$, the proof is similar. □

Theorem 2. *Fix* $I > 0$. *If* $n = 4$ *and* $\alpha > 0$, *or if* $n = 5$ *and* $\alpha = 1$, *then f can be chosen so that f satisfies (1) and the equilibrium is unstable.*

Proof. Taking $\alpha = 1$ simplifies the calculations because it allows us to consider the roots of $\widetilde{P}_n$, a degree $(n-1)$ polynomial, when determining stability rather than the roots of P_n, a degree n polynomial. So, in the case of $n = 4$ and $\alpha > 0$ as well as $n = 5$ and $\alpha = 1$, we need to localize the roots of a degree 4 polynomial. We may use the same technique in both cases. For this reason, the general case of $n = 4$, $\alpha > 0$ is similar to the case of $n = 5$, $\alpha = 1$ and, as in the proof of Theorem 1, we prove Theorem 2 only in the case $\alpha = 1$.

The main tool of the proof is the argument principle. Consider a contour in the complex plane which connects the points Ri and $-Ri$ via a semi-circle in the right half plane and a line on the imaginary axis. For large R, the dominant term of $\widetilde{P}_n$ on the semi-circle is of the form $R^{(n-1)} e^{(n-1)i\theta}$. So, in the limit as $R \to \infty$, the change in the argument on the semi-circle is $(n-1)\pi$. For $z \in \mathbb{C}$, let $\Re(z)$ denote the real part of z and $\Im(z)$ denote the imaginary part. We may determine the change in the argument on the imaginary axis between Ri and $-Ri$ by computing the zeros and tracking the signs of $\Re(\widetilde{P}_n(iy))$ and $\Im(\widetilde{P}_n(iy))$. For $n = 4$, the zeros of $\Re(\widetilde{P}_4(iy))$ satisfy

$$y^2 = \frac{(f(x_4) + 1)^2 - f'(x_4) I}{(f(x_4) + 3)(f(x_4) + 1)} =: r_{Re} > 0$$

and the zeros of $\Im(\widetilde{P}_4(iy))$ satisfy

$$y = 0 \quad \text{or} \quad y^2 = 2f(x_4) + 3 =: r_{Im} > 0.$$

To compute the change in the argument of on the imaginary axis, we track which quadrant of the complex plane $\widetilde{P}_4(iy)$ lies in as y varies from ∞ to $-\infty$. Note that $\Re(\widetilde{P}_4(iy)) = -C(y - \sqrt{r_{Re}})(y + \sqrt{r_{Re}})$ where C is a positive constant and $\Im(\widetilde{P}_4(iy)) = -y(y - \sqrt{r_{Im}})(y + \sqrt{r_{Im}})$. For y large, $\Re(\widetilde{P}_4(iy)) < 0$ and $\Im(\widetilde{P}_4(iy)) < 0$ so $\widetilde{P}_4(iy)$ lies in quadrant 3. $\Re(\widetilde{P}_4(iy))$ and $\Im(\widetilde{P}_4(iy))$ have only simple roots, so the quadrant changes exactly when y passes through one of the roots. The path $\widetilde{P}_4(iy)$ takes, and therefore the change in the argument, depends on whether $r_{Re} < r_{Im}$ or $r_{Im} < r_{Re}$. We consider these two cases separately.

Case 1: $r_{Im} < r_{Re}$

The number line below shows which quadrant of the complex plane $\widetilde{P}_4(iy)$ lies in.

$\widetilde{P}_4(iy)$ goes from $-i\infty$ to $i\infty$ as y goes from ∞ to $-\infty$ and, as the number line shows, makes no additional revolutions in between. That is, the change in the argument of on the imaginary axis is π. Along with

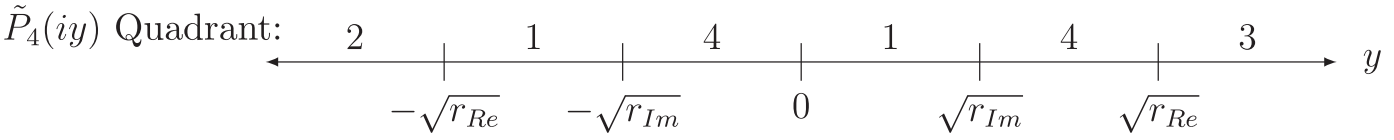

the change of 3π on the arc of the semi-circle, the total change in the argument of on the whole contour is 4π, indicating that there are 2 roots with positive real part when $r_{Im} < r_{Re}$.

Case 2: $r_{Re} < r_{Im}$

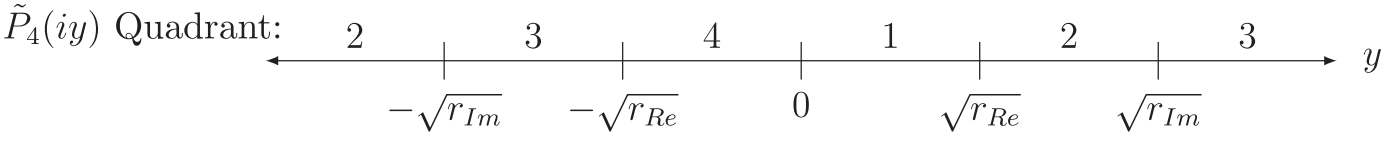

The change in the argument of on the imaginary axis is -3π in this case. The total change on the whole contour is then 0 and there are no roots inside the contour.

Let λ_4^* be a root of P_4 with largest real part. The analysis above shows that $\text{sign}(\Re(\lambda_4^*)) = \text{sign}(r_{Re} - r_{Im})$. Simplifying this expression, we have

$$\text{sign}(\Re(\lambda_4^*)) = \text{sign}(-f'(x_4)I - (2(f(x_4)+1)(f(x_4)+2)^2) \tag{5}$$

For $n = 5$ and $\alpha = 1$ we again compute the zeros of the real and imaginary parts of $\tilde{P}_n$ in order to determine which quadrant it lies in as it traverses the imaginary axis. The zeros of $\Re(\tilde{P}_5(iy))$ satisfy

$$2y^2 = (3f(x_5)+6) \pm \left[(3f(x_5)+6)^2 - 4\left(f(x_5)+1-\frac{f'(x_5)I}{f(x_5)+1}\right)\right]^{1/2}$$
$$=: 2r_{\pm}$$

and the zeros of $\Im(\tilde{P}_5(iy))$ satisfy

$$y = 0 \quad \text{or} \quad y^2 = \frac{3f(x_5)+4}{f(x_5)+4} =: r_{Im}$$

It can be shown that the change in the argument of $\tilde{P}_5(iy)$ as y goes from ∞ to $-\infty$ is -4π if and only if $r_{\pm} \in \mathbb{R}$ and $r_- < r_{Im} < r_+$. Further, if $r_{\pm} \in \mathbb{R}$, then $r_{Im} < r_+$ is always satisfied. Let λ_5^* be a root of P_5 with largest real part. Then, $\text{sign}(\lambda_5^*) \geq \text{sign}(r_- - r_{Im})$ which is equal to the sign of

$$-4f'(x_5)I - (f(x_5)+1)\left[\frac{4(3f(x_5)+4)(3f(x)+6)}{f(x_5)+4} - 4(f(x_5)+1) - \left(\frac{6f(x_5)+8}{f(x_5)+4}\right)^2\right]. \tag{6}$$

Now, fix $I > 0$ and pick any f satisfying (1). The equilibrium value is independent of network length, so let $\bar{x} = x_4 = x_5$. Now, if we have $\text{sign}(\Re(\lambda_4^*)) > 0$ and $\text{sign}(\Re(\lambda_5^*)) > 0$ then the equilibrium is unstable and we are done. If not, then we may choose g satisfying (1) with $g(\bar{x}) = f(\bar{x})$ so that the equilibrium value with g as the feedback function is the same, but with $|g'(\bar{x})|$ large enough so that $\text{sign}(\Re(\lambda_4^*)) > 0$ and $\text{sign}(\Re(\lambda_5^*)) > 0$, which guarantees the equilibrium is unstable. □

Theorem 3. *Let f satisfy (1), $I > 0$, and $\alpha = 1$. Let λ_4^* and λ_5^* be the roots of and $\tilde{P}_5$ with largest real part. If $\Re(\lambda_4^*) \geq 0$ then $\Re(\lambda_5^*) > 0$.*

Note that in particular, Theorem 3 says that for $\alpha = 1$, if the network with length 4 is unstable, then the network with length 5 is unstable as well.

Proof of Theorem 3. The steady state value of x_n is independent of n. So, the theorem is proved if the expression in (6) is strictly larger than the expression in (5). Letting $x = x_4 = x_5$, this requires

$$-4f'(x)I - (f(x)+1)\left[\frac{4(3f(x)+4)(3f(x)+6)}{f(x)+4} - 4(f(x)+1) - \left(\frac{6f(x)+8}{f(x)+4}\right)^2\right] > -f'(x)I - 2(f(x)+1)(f(x)+2)^2$$

Rearranging the inequality, we see this is true if and only if

$$-\left(\frac{6f(x)+8}{f(x)+4}\right)^2 < \frac{4}{f(x)+4}[2f(x)^3 + 8f(x)^2 + 15f(x) + 12]$$

The left hand side is negative and the right hand side is positive so the inequality is always satisfied. □

We now study stability in the case of general n. By applying Gershgorin's circle theorem (see, for example, [7]) to the Jacobian, we find a necessary condition for instability of the equilibrium, which is presented in the following proposition.

Proposition 1. *Let f satisfy (1) and fix I. Suppose the equilibrium is unstable. If $\alpha = 1$ then $-f'(x_n)I > f(x_n) + 1$. If $\alpha \neq 1$ then $-2f'(x_n)I > f(x_n) + \alpha$.*

The following theorem provides a sufficient condition for instability.

Theorem 4. *Let f satisfy (1) and fix I, $n \geq 4$, and $\alpha > 0$. Suppose that $-f'(x_n)I > 2(f(x_n)+\alpha)\left(\sec\left(\frac{3\pi}{2(n-1)}\right)\right)^{n-1}$ and $f(x_n) < \alpha$. Then for $m \geq n$, the equilibrium of the network with length m is unstable.*

Proof. We use notation and Theorems 1 and 2 of [8]. First, consider the network of length n. Let $Q_n(\lambda) = P_n(\lambda - 1)$ where P_n defined as in (4). P_n has a root with positive real part when Q_n has a root with real part greater than 1. Define $\gamma := -\frac{f'(x_n)I}{f(x_n)+\alpha}$. We may write

$$Q_n(\lambda) = (\lambda - 1 + \alpha)(\lambda^{n-1} + \gamma) + f(x_n)\lambda^{n-1}$$

and view $Q_n(\lambda)$ as a perturbation of $p(\lambda) := (\lambda - 1 + \alpha)(\lambda^{n-1} + \gamma)$. A root of p with largest real part is given by

$$\lambda^* := \gamma^{1/(n-1)} e^{i\pi/(n-1)}.$$

Let $Z(p, \varepsilon)$ be the root neighborhoods of p under the metric $d(p, q) = \max |a_j - b_j|/m_j$ with $m_{n-1} = 1$ and $m_j = 0$ for $j \neq n-1$ as defined in [8]. Let $Z^*(p, \varepsilon)$ be the connected component of $Z(p, \varepsilon)$ containing λ^*. By Theorem 2 of [8] there is at least one root of Q_n in $Z^*(p, f(x_n))$. So it is sufficient to show that

$$Z^*(p, f(x_n)) \subset \Omega := \left\{ z \in \mathbb{C} : \Re(z) > 1 \text{ and } \arg(z) \in \left(\frac{\pi}{2(n-1)}, \frac{3\pi}{2(n-1)} \right) \right\}.$$

First, we show that $\lambda^* \in \Omega$.

$$\begin{aligned} \Re(\lambda^*) &= \gamma^{1/(n-1)} \cos\left(\frac{\pi}{n-1}\right) \\ &> 2\left(\sec\left(\frac{3\pi}{2(n-1)}\right)\right)^{n-1} \cos\left(\frac{\pi}{n-1}\right) \\ &> 2\cos\left(\frac{\pi}{n-1}\right) \geq 1 \quad \text{for } n \geq 4 \end{aligned}$$

We also have $\arg(\lambda^*) = \frac{\pi}{2(n-1)}$ and thus $\lambda^* \in \Omega$. As $Z^*(p, f(x_n))$ is connected, the above containment holds if $\partial\Omega \cap Z(p, f(x_n)) = \varnothing$. Let $g(z) = p(z)/|z|^{n-1}$. By Theorem 1 of [8], $z \in Z(p, f(x_n))$ if and only if $|g(z)| \leq f(x_n)$.

Now suppose $z \in \partial\Omega$ with $\Re(z) = 1$ and $\arg(z) \in \left(\frac{\pi}{2(n-1)}, \frac{3\pi}{2(n-1)}\right)$. We have

$$|g(z)| = \frac{|z - 1 + \alpha||z^{n-1} + \gamma|}{|z|^{n-1}}.$$

$\Re(z) = 1$ so $z - 1 = \Im(z)i$ and thus $|z - 1 + \alpha| > \alpha$. Using the reverse triangle inequality we have

$$\begin{aligned} |g(z)| &> \alpha|1 - |z|^{-(n-1)}\gamma| \\ &\geq \alpha\left|1 - \left(\sec\left(\frac{3\pi}{2(n-1)}\right)\right)^{-(n-1)} \gamma\right| \\ &> \alpha|1 - 2| = \alpha > f(x_n) \end{aligned}$$

and we have $z \notin Z(p, f(x_n))$.

Now suppose $\arg(z) = \frac{\pi}{2(n-1)}$ and $\Re(z) \geq 1$. Then $z = re^{\frac{\pi i}{2(n-1)}}$ for $r \in \left[\sec\left(\frac{\pi}{2(n-1)}\right), \infty\right)$ and

$$\begin{aligned} \left|g\left(re^{\frac{\pi i}{2(n-1)}}\right)\right| &= r^{-(n-1)}\left|re^{\frac{\pi i}{2(n-1)}} - 1 + \alpha\right||r^{n-1}i + \gamma| \\ &> \left|re^{\frac{\pi i}{2(n-1)}} - 1 + \alpha\right| \\ &> \left|r\cos\left(\frac{\pi}{2(n-1)}\right) - 1 + \alpha\right| \geq \alpha > f(x_n) \end{aligned}$$

so $z \notin Z(p, f(x_n))$.

Finally, suppose $\arg(z) = \frac{3\pi}{2(n-1)}$ and $\Re(z) \geq 1$. Then $z = re^{\frac{3\pi i}{2(n-1)}}$ for $r \in \left[\sec\left(\frac{3\pi}{2(n-1)}\right), \infty\right)$ and

$$\begin{aligned} \left|g\left(re^{\frac{3\pi i}{2(n-1)}}\right)\right| &= r^{-(n-1)}\left|re^{\frac{3\pi i}{2(n-1)}} - 1 + \alpha\right||-ir^{n-1} + \gamma| \\ &> \left|re^{\frac{3\pi i}{2(n-1)}} - 1 + \alpha\right| \\ &> \left|r\cos\left(\frac{3\pi}{2(n-1)}\right) - 1 + \alpha\right| \geq \alpha > f(x_n) \end{aligned}$$

so again, $z \notin Z(p, f(x_n))$ and we have shown the case of $m = n$. For $m > n$, note that $\left(\sec\left(\frac{3\pi}{2(n-1)}\right)\right)^{n-1}$ is decreasing in n so that if the hypotheses are satisfied for $m = n$, they must also be satisfied for $m > n$. □

In practice, if we are given f, n, and α and we wish to know if there is an I for which the equilibrium is unstable, we may use (2) to solve for I as a function of x_n: $I = x_n(f(x_n) + \alpha)/f(x_n)$. Then the hypotheses of Proposition 1 and Theorem 4 can be written independent of I. Proposition 1 can then be used to find x_n for which stability is guaranteed and Theorem 4 can be used to find x_n for which instability is guaranteed. The corresponding values of I can be found by substituting x_n back into (2) (Fig. 4).

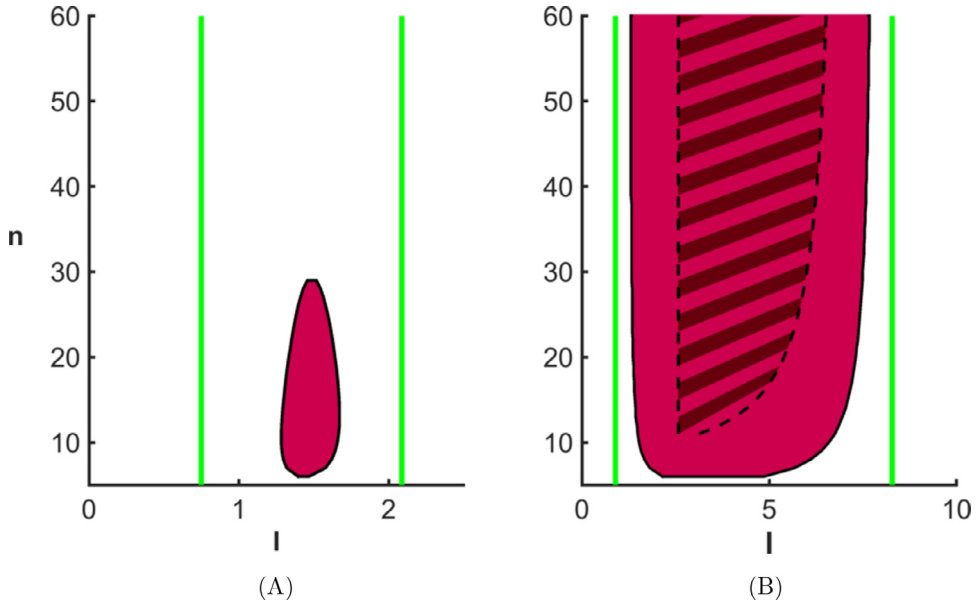

Fig. 4. Instability regions as a function of network length. A: The solid red area shows the instability region with $f(x) = \frac{10}{1+x^{10}} + 1/4$ and $\alpha = \frac{1}{50}$ computed numerically. $f(x) > \alpha$ for all x so Theorem 4 does not hold and if n is large enough the equilibrium is stable for every $I \in [0, \infty)$. Outside of the green lines, Proposition 1 applies so the equilibrium must be stable. B: $f(x)$ as in A but $\alpha = 1$ so that there are I for which Theorem 4 applies. The dark striped area shows where Theorem 4 guarantees instability and the solid red area shows where we have numerically calculated instabilities to occur. (For interpretation of the references to color in this figure legend, the reader is referred to the web version of this article.)

3. A special case

To better understand how the properties of f affect the system, we consider a particular form of f when $n = 4$. Consider f of the form

$$f(x) = \begin{cases} A + C, & x < 0 \\ A + C - sx, & 0 \le sx \le A \\ C, & sx > A \end{cases} \tag{7}$$

where $A > C$, $s > 0$, and $C \ge 0$. Let $f_h(x) = f(x - h)$ for $h \ge 0$. We will examine how varying C, s, and h effect the instability region and amplitude of limit cycles when $n = 4$ and $\alpha = 1$. We provide two theorems. To state the theorems, we define $I_1 = \inf\{I > 0: x(I)\text{isunstable}\}$ and $I_2 = \sup\{I > 0: x(I)\text{isunstable}\}$ and note that (I_1, I_2) is the instability region. The first theorem relates the parameters of f_h with the existence of the instability region. The second theorem shows that when the instability region is not empty, $|x_4(I_2) - x_4(I_1)|$ must be relatively small. The purpose of the second theorem is to show that the region of instability is contained in the homeostatic region.

Theorem 5. *Define $f_h(x)$ as above, let $n = 4$ and $\alpha = 1$. Let $C^* > 0$ satisfy $2C^*(C^* + 2)^2 = A + sh$. If $C > C^*$ then the equilibrium is stable for every $I \in [0, \infty)$. If $0 < C < C^*$, then the instability region is nonempty and $I_2 < \infty$. If $C = 0$ then the instability region is nonempty and $I_2 = \infty$.*

Proof. First note that if $x_4 < h$ or $s(x_4 - h) > A$ then $f_h'(x_4) = 0$ and by Proposition 1, the equilibrium is stable.

Let $g(x) = sx - 2(A + C - s(x - h))(A + C + 2 - s(x - h))^2$.

For $x_4 \in (h, A/s + h)$, applying Eq. (5) from the proof of Theorem 2 shows that the equilibrium is stable if $g(x_4) < 0$ and unstable if $g(x_4) > 0$. Note that g is strictly monotone increasing and $g(A/s + h) = (A + sh) - 2C(2 + C)^2$.

Suppose $C > C^*$. Then $g(x) < g(A/s + h) < 0$ for all $x \in (h, A/s + h)$ so that the equilibrium is stable for every $I \ge 0$.

Now suppose $C < C^*$. Then $g(A/s + h) > 0$ so there is an interval $U \subset (h, A/s + h)$ so that if $x_4 \in U$ then $g(x_4) > 0$ and the equilibrium is unstable. If, in addition, $C > 0$, then the proof of Lemma 1 still works and $x_4 \to \infty$ as $I \to \infty$ so that there is an I for which $x_4 > A/s + h$ and stability is regained. In this case I_2 satisfies $x_4(I_2) = A/s + h$.

On the other hand, if $C = 0$, then as in Lemma 1, x_4 satisfies $\ell(x_4) := (f(x_4) + 1)x_4/f(x_4) = I$. Because $f(x) \to 0$ as $x \to A/s + h$, we see that $\ell(x) \to \infty$ as $x \to A/s + h$ and $\ell: [0, A/s + h) \to [0, \infty)$ is invertible. Thus we always have $x_4 < A/s + h$, so stability is not regained and $I_2 = \infty$. □

Theorem 6. *Define $f_h(x)$ as above, let $n = 4$ and $\alpha = 1$. Suppose the instability region is nonempty. Then $x_4(I_1) > \frac{8}{9}x_4(I_2)$.*

Proof.

Define $g(x, C) = sx - 2(A + C - s(x - h))(A + C + 2 - s(x - h))^2$.

This is the same g as in the proof of Theorem 5 except that we make the dependence on C explicit. We know that the equilibrium is stable when $g < 0$ and unstable when $g > 0$. Note that g is decreasing in C, so we have $g(x, C) < g(x, 0)$. We also have $x_4(I_2) = A/s + h$. Letting $\kappa = \frac{1}{9}$, we have

$$\begin{aligned} g\left(\frac{8}{9}x_4(I_2), 0\right) &= g((1 - \kappa)(A/s + h), 0) \\ &= (1 - \kappa)A + (1 - \kappa)sh - 2(\kappa A + \kappa sh)(\kappa A + \kappa sh + 2)^2 \\ &\le (1 - \kappa)A - 2\kappa A(\kappa A + 2)^2 \\ &= (1 - \kappa)A - 2(\kappa A)^3 - 8\kappa A^2 - 8\kappa A \\ &< A - 9\kappa A = 0 \end{aligned}$$

The instability region is nonempty so I_1 exists and $x_4(I_1)$ satisfies $g(x_4(I_1), C) = 0$. However, g is increasing in x and we have shown that $g(\frac{8}{9}x_4(I_2), C) < 0$ so we must have $x_4(I_1) \in \left(\frac{8}{9}x_4(I_2), x_4(I_2)\right)$ as claimed. □

Theorem 6 says that although $|I_2 - I_1|$ may be large, the value of x_4 doesn't change very much on that interval. This indicates that the instability region lies on the homeostatic plateau. For example, Fig. 5A shows that for $C = 1/5$, $I_1 \approx 25$ while $I_2 \approx 100$, but $x_4(I_1)$ and $x_4(I_2)$ are still close to each other.

Finally, we present numerical calculations of the instability regions and limit cycle amplitudes as C, s, and h are individually varied. Fig. 5 shows the instability regions. Fig. 6 shows the maximum limit cycle

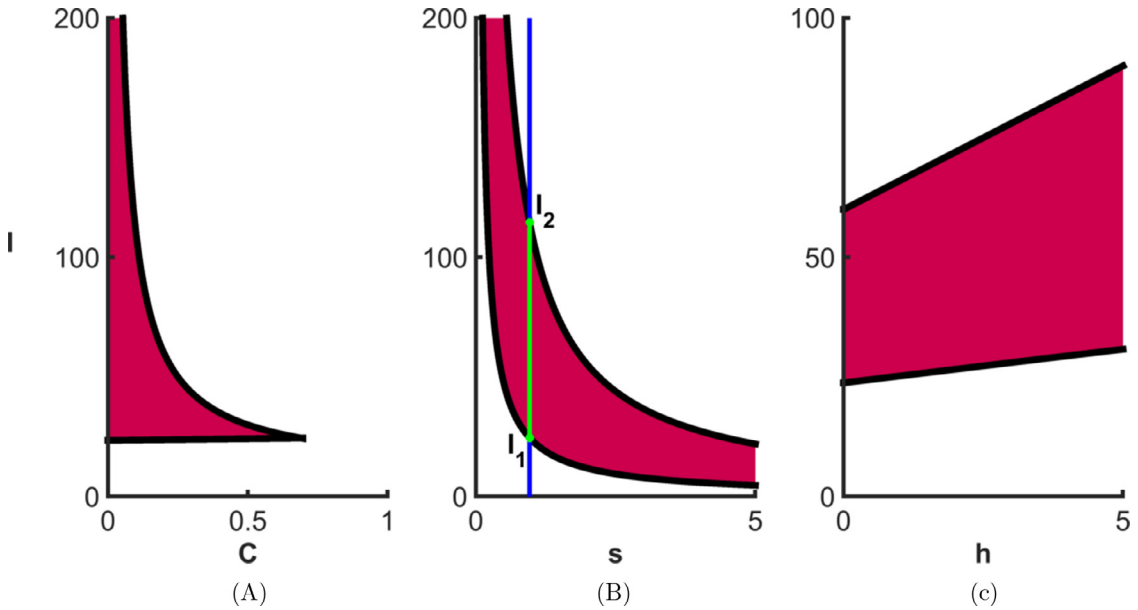

Fig. 5. Parameter dependence of the instability region. $f_h(x)$ is chosen as above with $A = 10$, $C = 1/5$, $s = 1$, and $h = 0$ except when they are varied. The solid red regions show the numerically calculated instability regions. A: When $A = 10$ and $h = 0$, $C^* \approx 0.69$. As $C^* \to 0$, $I_2 \to \infty$. B: Increasing s decreases both I_1 and I_2. The line $s = 0.96$ has been plotted and indicates for which values of I the equilibrium is stable (blue), and for which values of I there is a limit cycle (green). I_1 and I_2 are the intersection points of the line $s = 0.96$ and the boundary of the instability region as indicated. For small s, $A/s + h$ is very large, causing I_2 to be very large. C: Increasing h increases the size of the instability region. (For interpretation of the references to color in this figure legend, the reader is referred to the web version of this article.)

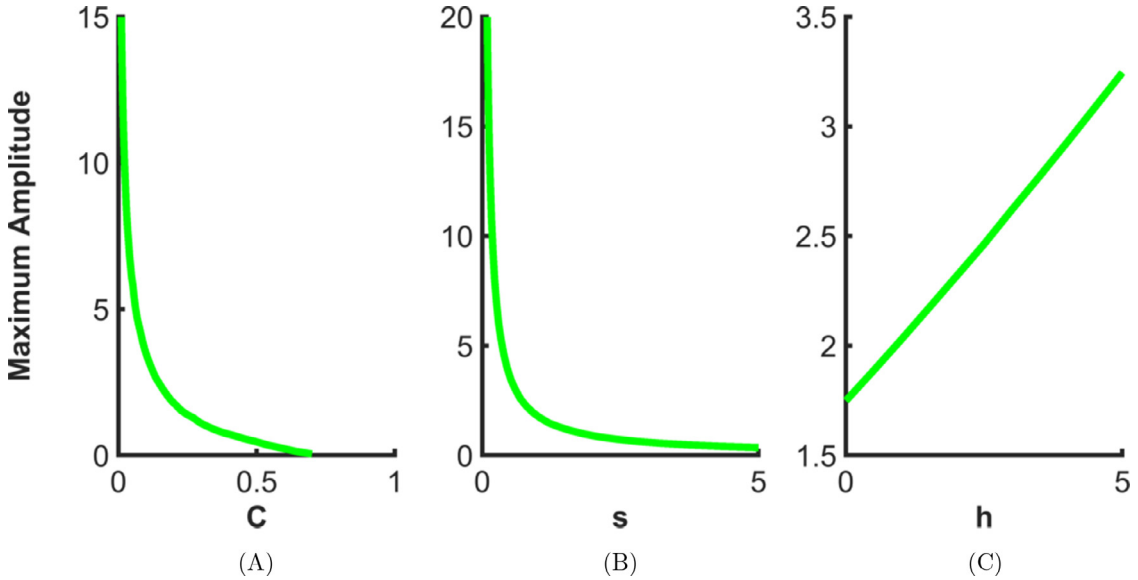

Fig. 6. Parameter dependence of the limit cycle amplitudes. The maximum amplitude of the limit cycles over the instability region is calculated numerically and plotted as a function of the parameters of f_h. The parameters are fixed at $A = 10$, $s = 1$, $C = 1/5$, and $h = 0$ when they are not varied. The maximum amplitudes appear to be proportional to the size of the instability region. By amplitude, we mean the minimum of x_4 subtracted from the maximum over the limit cycle.

amplitude over the instability region. We choose A large enough so that $x_4(I_1) > h$.

4. Discussion

Gene expression levels vary by roughly 25% from individual to individual [9,10]. Furthermore, many genes that code for enzymes have polymorphisms with high frequency in the human population that are functional in the sense that they raise or lower the activity of the enzyme by 20% to 80% (see, for example, Table 1 in [11]). How do cellular and physiological systems cope with this enormous biological variation? The answer is that there is a myriad of homeostatic mechanisms that reduce the effects of gene expression differences and gene polymorphisms. Some of these mechanisms operate at the gene level, some operate at the biochemical level, and some at the physiological level. But many also operate between levels, because biochemical substrates affect gene expression levels as do physiological variables such as hormones. These homeostatic regulations should not be thought of as a separate layer of regulation since they probably evolved simultaneously with the genetic, biochemical, and physiological systems. They are integral parts of the whole system and must be investigated in order to understand cell biology and whole body physiology.

It is well known that feedback inhibition with explicit time delays can produce oscillations in mechanical or biological systems. In the case of feedback inhibition in a biochemical chain, there is no explicit time delay, but a time delay is implicit in the length of the chain, n. As we have shown, the existence of an input interval (I_1, I_2) in which there are oscillations, the length of the interval, and the size of the oscillations depends in interesting and complicated ways on the properties of the inhibition function, f, the length of the chain, and the size of the leakage parameter, α. Our main point is that when the amplitudes of the oscillations are relatively small, one maintains the homeostatic plateau and the chair shape despite the instability of the equilibrium and the limit cycle oscillations.

This phenomenon is not confined to the homeostatic mechanism of feedback inhibition. In [5] (Fig. 9), we introduced the parallel

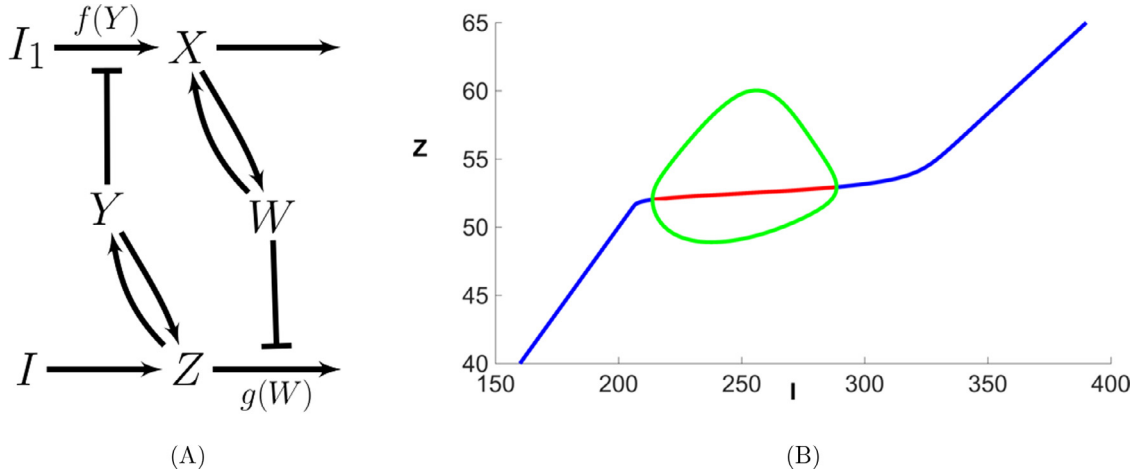

Fig. 7. Homeostasis despite instability in the parallel inhibition motif. The network is shown in Panel A. All reactions are linear mass action except for the two inhibitions given by f and g. Panel B shows the instability region in red and the maximum amplitude of the limit cycle oscillations in green. The amplitude of the oscillations can be adjusted by changing parameters. The differential equations and the explicit formulas for f and g are available from the authors. (For interpretation of the references to color in this figure legend, the reader is referred to the web version of this article.)

inhibition motif and showed that it can produce the classic chair shape with a homeostatic plateau and escape from homeostasis. It is easy to prove that the two-variable implementation of the parallel inhibition motif given in [5] has a stable equilibrium for all inputs *I*. However, consider the four-variable implementation of the parallel inhibition motif given in Fig. 7, Panel A. Each of the inhibitions acts through an intermediate variable (*Y* or *W*), and, as can be seen in Panel B, the homeostatic variable, *Z*, shows the phenomenon we study in this paper. For more discussion of the parallel inhibition motif and an explicit biological example, see [5].

This paper introduces a mathematically new low codimension phenomenon in network dynamics - the coexistence of Hopf bifurcation with homeostasis. Both of these singularities occur on variation of *I*, which simultaneously serves the roles of input parameter and bifurcation parameter. Infinitesimal chairs [6] have codimension one and the co-existence with Hopf bifurcation has codimension two. However, the existence of codimension two phenomena should not be surprising in biochemical networks which have many parameters (rate constants and the like). Note that Fig. 3 suggests a degenerate Hopf bifurcation [12,13] where a pair of Hopf bifurcations merge and disappear coupled with an infinitesimal chair, which is a codimension three phenomenon. Theoretically, the coexistence of homeostasis with bifurcation is a fascinating mathematical problem that should lead to new and interesting network issues. For example, another codimension three interaction is that of a hysteresis point [13] with a chair singularity. Such an interaction might lead to the coexistence of two plateaus with the possibility of a new form of switching. In any case, understanding the theoretical structure of these mathematical interactions will be a subject of future study.

Competing interest

The authors declare that they have no competing interests.

Authors' contributions

The phenomenon of homeostasis despite instability was discovered by Best and the mathematical calculations were done by Duncan. Nijhout and Reed organized the project and Golubitsky contributed the perspective of singularity theory. The paper was written by Best, Duncan, and Reed, and was read and approved by all authors.

Acknowledgements

This research was supported by National Institutes of Health grants 1R01MH106563-01A1(JAB,MCR,HFN) and 1R21MH109959-01A1 (JAB,MCR,HFN) and NSF grants IOS-1562701 (HFN), EF-1038593 (HFN,MCR), IOS-1557341 (HFN,MCR).

References

[1] H.F. Nijhout, J. Best, M. Reed, Escape from homeostasis, Math. Biosci. 257 (2014) 104–110.
[2] H.F. Nijhout, M. Reed, Homeostasis and dynamic stability of the phenotype link robustness and stability, Int. Comp. Biol. 54 (2014) 264–275.
[3] I. Sgouralis, A. Layton, Control and modulations of fluid flow in the rat kidney, Bull. Math. Biol. 75 (2013) 2551–2574.
[4] N. Green, L. Lee, Modern and evolving understanding of cerebral perfusion and autoregulation, Adv. Anesthesia 30 (2012) 97–129.
[5] M. Reed, J. Best, M. Golubitsky, I. Stewart, H.F. Nijhout, Analysis of homeostatic mechanisms in biochemical networks, Bull. Math. Biol. 79 (2017) 2534–2557.
[6] M. Golubitsky, I. Stewart, Homeostasis, singularities and networks, J. Math. Biol. 1 (2016). doi 10.1007/s00285–016–1024–2 .
[7] R.S. Varga, Matrix Iterative Analysis, Computational Mathematics, Springer, New York, NY, 2000.
[8] R. Mosier, Root neighborhoods of a polynomial, Math. Comput. 47 (1986) 265–273.
[9] M. Oleksiak, G. Churchill, D. Crawford, Variation in gene expression within and among natural populations, Nat. Genet. 32 (2002) 261–266.
[10] A. Whitney, M. Diehn, S. Popper, A. Alizadeh, J. Boldrick, D. Relman, P. Brown, Individuality and variation in gene expression patterns in human blood, PNAS 100 (2003) 1896–1901.
[11] H.F. Nijhout, J. Best, M. Reed, Using mathematical models to understand metabolism, genes and disease, BMC Biol. 13 (2015). 79–
[12] M. Golubitsky, W. Langford, Classification and unfoldings of degenerate hopf bifurcation, J. Diff. Eqns. 41 (1981) 375–415.
[13] M. Golubitsky, D. Schaeffer, Singularities and Groups in Bifurcation Theory: Vol. I, Applied Mathematical Sciences 51, Springer-Verlag, New York, NY, 1985.